

Fig. 15. The equivalent plastic strain and phase field at different times under the impact velocity  $v = 10$  m/s by mesh 4.

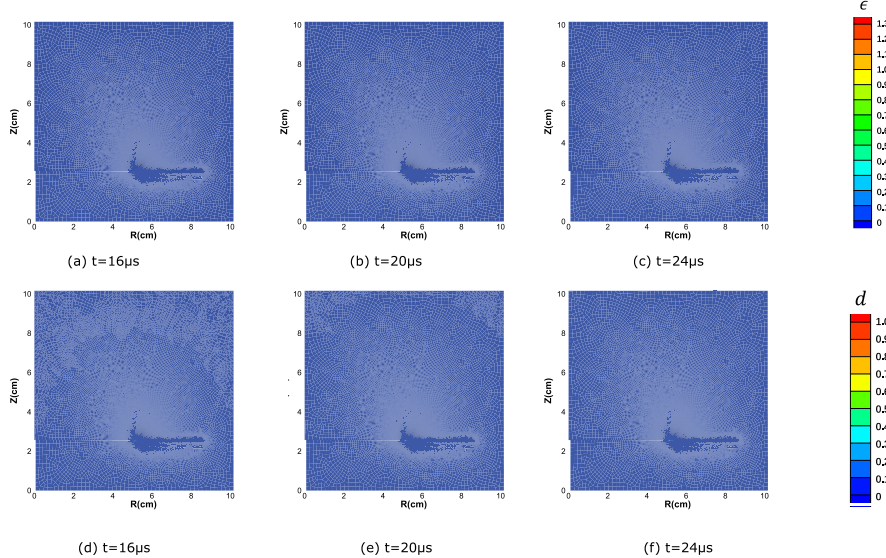


Fig. 16. The equivalent plastic strain and phase field at different times under the impact velocity  $v = 40$  m/s by mesh 4.

## Appendix. The setup of the sensitivity analysis

Here, the setup of the global sensitivity analysis for the impact of two plates is provided in detail.

In the ideal case, this analysis requires solving the problem many times. In order to alleviate the time-consuming finite element calculation, a surrogate model based on the polynomial chaos expansion (PCE) [57] with the Latin hypercube sampling method [58] is adopted. One advantage of the PCE-based Sobol' method is that the Sobol' indices can be analytically acquired by the coefficients of PCE [57,59] almost without extra computations.

The entire analysis is performed with the UQLab package [60], a MATLAB-based uncertainty quantification framework. The uncertain parameters are listed in Table A.1.

The basic procedure of performing the sensitivity analysis is listed below:

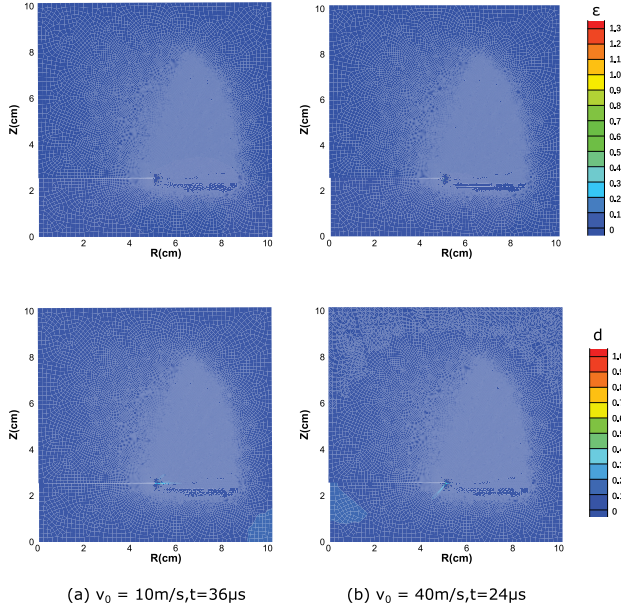


**Fig. 17.** The equivalent plastic strain and phase field with  $\chi = 0$ .

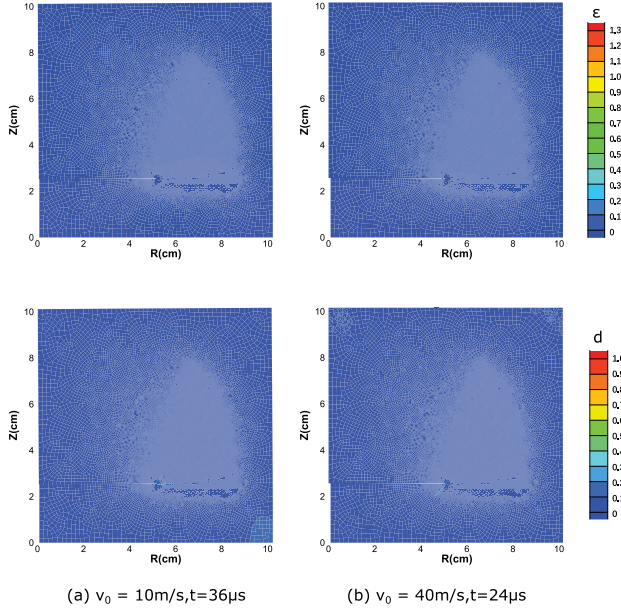


**Fig. 18.** The equivalent plastic strain and phase field with  $\chi = 0.5$ .

Step 1: Define and generate the input parameters by Latin hypercube sampling method. Here, the total number of sampling points is  $N = 120$ , of which 100 are used to calculate the coefficients of the PCE, which is enough to acquire accurate coefficients [57] empirically, and the remaining 20 are used as a validation set for the setup of the PCE models.

Step 2: Perform the finite element computations using the data of the sampling points as inputs, and extract the corresponding outputs.

Step 3: Calculate the coefficients of the third-order PCE model by the inputs and outputs based on the ordinary least squares method.

Step 4: Analytically estimate the second-order Sobol' indices by the coefficients of PCE, and visualize the Sobol' indices.

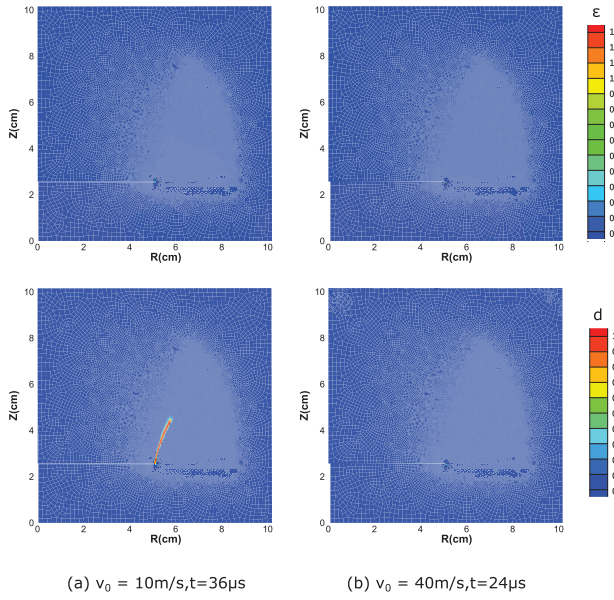


**Fig. 19.** The equivalent plastic strain and phase field with  $\chi = 0.7$ .

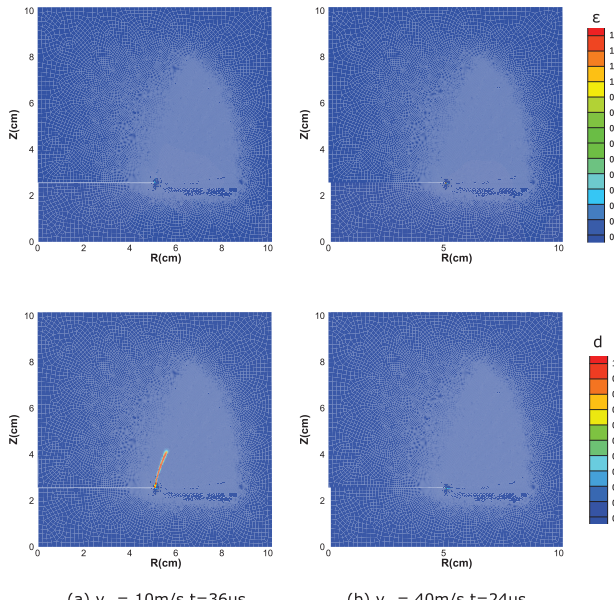


**Fig. 20.** The equivalent plastic strain and phase field with  $\chi = 0.8$ .

**Table A.1**  
The uncertain input parameters.

Parameter	Distribution type	Unit	Mean/ Lower bound	Standard deviation/ Upper bound
$g_c^{\text{vol}}$	Normal	N/mm	0.88	0.1
$g_c^{\text{dev}}$	Normal	N/mm	22	2.2
$\chi$	Uniform	—	0.5	1

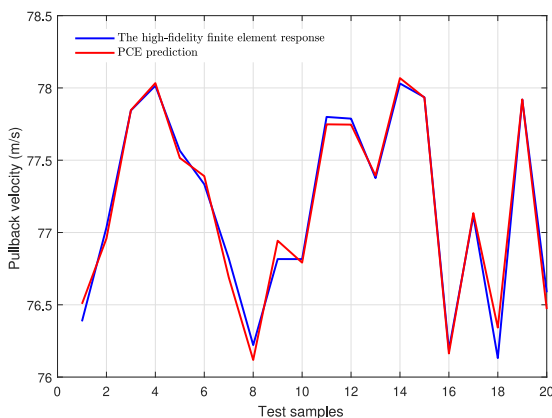


**Fig. A.21.** The pullback velocity of right end surface from the high-fidelity finite element responses and predictions by the PCE model. The maximum absolute error is 0.1307 m/s, which is 0.17% of the maximum value of the high-fidelity finite element response among the samples.

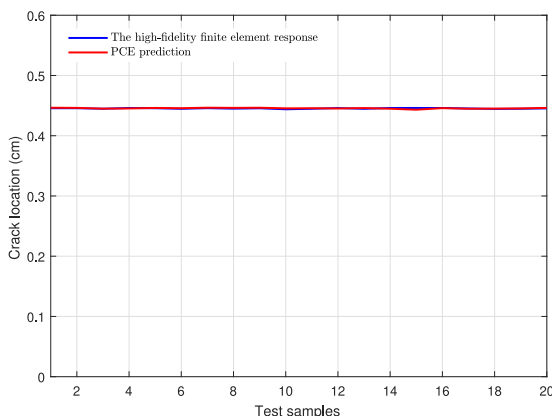


**Fig. A.22.** The crack location from the high-fidelity finite element responses and predictions by the PCE model. The maximum absolute error is 0.0029 cm, which is 0.65% of the maximum value of the high-fidelity finite element response among the samples.

In the above process, the finite element computations (Step 2) are the most time-consuming, and the time for the remaining parts is negligible.

Figs. A.21 and A.22 plot the pullback velocity of the right end surface and the crack location predicted from the finite element computations and the PCE model for the 20 sampling points from the validation set to verify the setup of the PCE model. From these figures, we see that there is only a tiny difference between the high-fidelity finite element response and the predictions, which shows that it is appropriate to substitute the high-fidelity finite element model by the PCE model setup.

## References

- [1] Goldsmith W. Impact. Courier Corporation; 2001.
- [2] Camacho GT, Ortiz M. Computational modelling of impact damage in brittle materials. *Int J Solids Struct* 1996;33(20–22):2899–938.
- [3] Børvik T, Hopperstad O, Berstad T, Langseth M. A computational model of viscoplasticity and ductile damage for impact and penetration. *Eur J Mech A Solids* 2001;20(5):685–712.
- [4] Thornton C, Yin K, Adams M. Numerical simulation of the impact fracture and fragmentation of agglomerates. *J Phys D: Appl Phys* 1996;29(2):424.
- [5] Li S, Liu W-K, Qian D, Guduru PR, Rosakis AJ. Dynamic shear band propagation and micro-structure of adiabatic shear band. *Comput Methods Appl Mech Engrg* 2001;191(1–2):73–92.
- [6] Li S, Liu WK, Rosakis AJ, Belytschko T, Hao W. Mesh-free Galerkin simulations of dynamic shear band propagation and failure mode transition. *Int J Solids Struct* 2002;39(5):1213–40.
- [7] Rabczuk T, Belytschko T. Cracking particles: A simplified meshfree method for arbitrary evolving cracks. *Internat J Numer Methods Engrg* 2004;61(13):2316–43.
- [8] Rabczuk T, Belytschko T. A three-dimensional large deformation meshfree method for arbitrary evolving cracks. *Comput Methods Appl Mech Engrg* 2007;196(29):2777–99.
- [9] Ren H, Zhuang X, Cai Y, Rabczuk T. Dual-horizon peridynamics. *Internat J Numer Methods Engrg* 2016;108(12):1451–76.
- [10] Bourdin B, Francfort GA, Marigo J-J. Numerical experiments in revisited brittle fracture. *J Mech Phys Solids* 2000;48(4):797–826.
- [11] Francfort GA, Marigo J-J. Revisiting brittle fracture as an energy minimization problem. *J Mech Phys Solids* 1998;46(8):1319–42.

- [12] Ambati M, Gerasimov T, De Lorenzis L. A review on phase-field models of brittle fracture and a new fast hybrid formulation. *Comput Mech* 2015;55(2):383–405.
- [13] Wu J-Y, Nguyen VP, Nguyen CT, Sutula D, Sinaie S, Bordas SP. In: Bordas SP, Balint DS, editors. Chapter one - Phase-field modeling of fracture. *Advances in applied mechanics*, vol. 53. Elsevier; 2020, p. 1–183.
- [14] Bourdin B, Francfort GA. Past and present of variational fracture. *SIAM News* 2019;52(9).
- [15] Francfort G. Variational fracture: Twenty years after. *Int J Fract* 2021;1–11.
- [16] Nguyen VP, Wu J-Y. Modeling dynamic fracture of solids with a phase-field regularized cohesive zone model. *Comput Methods Appl Mech Engrg* 2018;340:1000–22.
- [17] Wu J-Y. A unified phase-field theory for the mechanics of damage and quasi-brittle failure. *J Mech Phys Solids* 2017;103:72–99.
- [18] Zhou S, Rabczuk T, Zhuang X. Phase field modeling of quasi-static and dynamic crack propagation: COMSOL implementation and case studies. *Adv Eng Softw* 2018;122:31–49.
- [19] Ren H, Zhuang X, Anitescu C, Rabczuk T. An explicit phase field method for brittle dynamic fracture. *Comput Struct* 2019;217:45–56.
- [20] Mandal TK, Nguyen VP, Wu J-Y. Evaluation of variational phase-field models for dynamic brittle fracture. *Eng Fract Mech* 2020;235:107169.
- [21] Zhang H, Peng H, Pei X-Y, Li P, Tang T-G, Cai L-C. A phase-field model for spall fracture. *J Appl Phys* 2021;129(12):125903.
- [22] Miehe C, Hofacker M, Schänzel L-M, Aldakheel F. Phase field modeling of fracture in multi-physics problems. part II. coupled brittle-to-ductile failure criteria and crack propagation in thermo-elastic-plastic solids. *Comput Methods Appl Mech Engrg* 2015;294:486–522.
- [23] McAuliffe C, Waisman H. A unified model for metal failure capturing shear banding and fracture. *Int J Plast* 2015;65:131–51.
- [24] McAuliffe C, Waisman H. A coupled phase field shear band model for ductile–brittle transition in notched plate impacts. *Comput Methods Appl Mech Engrg* 2016;305:173–95.
- [25] Borden MJ, Hughes TJ, Landis CM, Anvari A, Lee IJ. A phase-field formulation for fracture in ductile materials: Finite deformation balance law derivation, plastic degradation, and stress triaxiality effects. *Comput Methods Appl Mech Engrg* 2016;312:130–66.
- [26] Ambati M, Kruse R, De Lorenzis L. A phase-field model for ductile fracture at finite strains and its experimental verification. *Comput Mech* 2016;57(1):149–67.
- [27] Chu D, Li X, Liu Z, Cheng J, Wang T, Li Z, et al. A unified phase field damage model for modeling the brittle-ductile dynamic failure mode transition in metals. *Eng Fract Mech* 2019;212:197–209.
- [28] Wang T, Liu Z, Cui Y, Ye X, Liu X, Tian R, et al. A thermo-elastic-plastic phase-field model for simulating the evolution and transition of adiabatic shear band. Part I. Theory and model calibration. *Eng Fract Mech* 2020;107028.
- [29] Wang T, Liu Z, Cui Y, Ye X, Liu X, Tian R, et al. A thermo-elastic-plastic phase-field model for simulating the evolution and transition of adiabatic shear band. Part II. Dynamic collapse of thick-walled cylinder. *Eng Fract Mech* 2020;107027.
- [30] Zhang H, Pei X-Y, Peng H, Wu J-Y. Phase-field modeling of spontaneous shear bands in collapsing thick-walled cylinders. *Eng Fract Mech* 2021;107706.
- [31] Simo JC, Hughes TJR. *Computational Inelasticity*. New York: Springer Verlag; 1998.
- [32] McAuliffe C, Waisman H. On the importance of nonlinear elastic effects in shear band modeling. *Int J Plast* 2015;71:10–31.
- [33] Brepols T, Vladimirov IN, Reese S. Numerical comparison of isotropic hypo-and hyperelastic-based plasticity models with application to industrial forming processes. *Int J Plast* 2014;63:18–48.
- [34] Amor H, Marigo J-J, Maurini C. Regularized formulation of the variational brittle fracture with unilateral contact: Numerical experiments. *J Mech Phys Solids* 2009;57(8):1209–29.
- [35] Miehe C, Welschinger F, Hofacker M. Thermodynamically consistent phase-field models of fracture: Variational principles and multi-field FE implementations. *Internat J Numer Methods Engrg* 2010;83(10):1273–311.
- [36] Wu J-Y, Nguyen VP, Zhou H, Huang Y. A variationally consistent phase-field anisotropic damage model for fracture. *Comput Methods Appl Mech Engrg* 2020;358:112629.
- [37] Liu Y, Cheng C, Ziae Rad V, Shen Y. A micromechanics-informed phase field model for brittle fracture accounting for unilateral constraint. *Eng Fract Mech* 2021;241:107358.
- [38] Miehe C, Hofacker M, Welschinger F. A phase field model for rate-independent crack propagation: Robust algorithmic implementation based on operator splits. *Comput Methods Appl Mech Engrg* 2010;199(45–48):2765–78.
- [39] Benson DJ. Computational methods in Lagrangian and Eulerian hydrocodes. *Comput Methods Appl Mech Engrg* 1992;99(2–3):235–394.
- [40] Zukas J. *Introduction to Hydrocodes*. Elsevier; 2004.
- [41] Wilkins M. Calculation of elastic-plastic flow. *Methods Comput Phys* 1964;3:211–63.
- [42] Hallquist JO. *LS-DYNA Theory Manual*. Livermore, CA: Livermore Software Technology Corporation; 2006.
- [43] Johnson GR, Cook WH. A constitutive model and data for metals subjected to large strains, high strain rates and high temperatures. In: Proceedings of the 7th international symposium on ballistics, vol. 21. 1983. p. 541–547.
- [44] Steinberg DJ, Cochran SG, Guinan M. A constitutive model for metals applicable at high-strain rate. *J Appl Phys* 1980;51(3):1498–504.
- [45] Von Neumann J, Richtmyer RD. A method for the numerical calculation of hydrodynamic shocks. *J Appl Phys* 1950;21(3):232–7.
- [46] Flanagan DP, Belytschko T. A uniform strain hexahedron and quadrilateral with orthogonal hourglass control. *Internat J Numer Methods Engrg* 1981;17(5):679–706.
- [47] Rittel D, Zhang L, Osovski S. The dependence of the Taylor-Quinney coefficient on the dynamic loading mode. *J Mech Phys Solids* 2017;107:96–114.
- [48] Hu C-M, He H-L, Hu S-S. Research on the spalling of 45# steel under different strain rate. *J Exp Mech* 2003;18(2):246–50.
- [49] Li Y-C, Cao J-D, Dong J, Yao L. Research of damage evolution equation and spallation criterion of 45# steel. *Chin Q Mech* 2006;2.
- [50] Hamdia KM, Silani M, Zhuang X, He P, Rabczuk T. Stochastic analysis of the fracture toughness of polymeric nanoparticle composites using polynomial chaos expansions. *Int J Fract* 2017;206(2):215–27.
- [51] Liang B, Mahadevan S. Error and uncertainty quantification and sensitivity analysis in mechanics computational models. *Int J Uncertain Quantif* 2011;1(2).
- [52] Sobol' IM. On sensitivity estimation for nonlinear mathematical models. *Mat Model* 1990;2(1):112–8.
- [53] Kalthoff JF. Shadow optical analysis of dynamic shear fracture. *Opt Eng* 1988;27(10):271035.
- [54] Kalthoff JF. Failure methodology of mode-II loaded cracks. *Strength Fract Complex* 2003;1(3):121–38.
- [55] Zhou M, Rosakis AJ, Ravichandran G. Dynamically propagating shear bands in impact-loaded prenotched plates—I. Experimental investigations of temperature signatures and propagation speed. *J Mech Phys Solids* 1996;44(6):981–1006.
- [56] Zhou M, Ravichandran G, Rosakis AJ. Dynamically propagating shear bands in impact-loaded prenotched plates—II. Numerical simulations. *J Mech Phys Solids* 1996;44(6):1007–32.
- [57] Sudret B. Global sensitivity analysis using polynomial chaos expansions. *Reliab Eng Syst Saf* 2008;93(7):964–79.
- [58] Iman RL, Conover W-J. A distribution-free approach to inducing rank correlation among input variables. *Comm Statist Simulation Comput* 1982;11(3):311–34.
- [59] Crestaux T, Le Maître O, Martinez J-M. Polynomial chaos expansion for sensitivity analysis. *Reliab Eng Syst Saf* 2009;94(7):1161–72.
- [60] Marelli S, Sudret B. UQLab: A framework for uncertainty quantification in Matlab. In: *Vulnerability, uncertainty, and risk: Quantification, mitigation, and management*. American Society of Civil Engineers; 2014, p. 2554–63.